Spin-flip excitations, spin waves, and magnetoexcitons in graphene Landau levels at integer filling factors

R. Roldán,[1,2] J.-N. Fuchs,[2] and M. O. Goerbig[2]

[1]*Institute for Molecules and Materials, Radboud University Nijmegen, Heyendaalseweg 135, 6525 AJ Nijmegen, The Netherlands*
[2]*Laboratoire de Physique des Solides, Univ. Paris-Sud–CNRS, UMR 8502, F-91405 Orsay Cedex, France*

We study collective electronic excitations in graphene in the integer quantum-Hall regime, concentrating mainly on excitations with spin reversal such as spin-flip and spin-wave excitations. We show that these excitations are correctly accounted for in the time-dependent Hartree-Fock and strong magnetic field approximations, in contrast to spin-conserving (magnetoexciton) modes which involve a strong Landau-level mixing at nonzero wave vectors. The collective excitations are discussed in view of prominent theorems, such as Kohn's and Larmor's. Whereas the latter remains valid in graphene and yields insight into the understanding of spin-dependent modes, Kohn's theorem does not apply to relativistic electrons in graphene. We finally calculate the exchange correction to the chemical potential in the weak magnetic field limit.

I. INTRODUCTION

The role of electron-electron interactions in graphene [two-dimensional (2D) graphite] is still a debated issue. Whereas most of its electronic properties can be understood within a model of 2D noninteracting massless Dirac fermions,[1] there are some experimental indications for the presence of Coulomb interactions.[2] These correlations, which may be quantified by the graphene fine-structure constant $\alpha_G = e^2/\hbar \varepsilon v_F \simeq 2.2/\varepsilon$, in terms of the Fermi velocity v_F and the dielectric constant ε, seem, however, to be weak and long ranged. Therefore, strongly correlated phases that are expected in the large-α_G limit[3] or for short-range Hubbard interactions[4–6] are unlikely to occur in undoped or moderately doped graphene. Theoretically, a perturbative Fermi-liquid-type treatment of the Coulomb interactions yields a logarithmic divergence of the Fermi velocity,[7] a renormalization of thermodynamic quantities such as the compressibility[8] as well as to a control of the orbital magnetic susceptibility.[9]

The situation is different if the graphene electrons are exposed to a strong magnetic field that quantizes their kinetic energy into nonequidistant Landau levels (LLs), $\epsilon_n = (\lambda \hbar v_F / l_B) \sqrt{2n}$, where $\lambda = \pm 1$ is the band index, $l_B = \sqrt{\hbar c/eB}$ is the magnetic length, and n denotes the LL index.[1] The most prominent consequence of this relativistic LL quantization and the presence of a zero-energy LL for $n=0$ is a peculiar integer quantum-Hall effect (QHE), with an unusual sequence of Hall plateaus.[10,11] The LLs are highly degenerate, as in the usual 2D electron gas (2DEG) with a parabolic band dispersion, where the density of states per LL (and per unit area) is given by the flux density $n_B = 1/2\pi l_B^2 = eB/h$, which is proportional to the perpendicular magnetic field. The filling of the LLs is then characterized by the ratio (filling factor) $\nu = n_{el}/n_B$ between the 2D electronic density n_{el} and n_B. A partially filled LL may then be viewed as a strongly correlated electron system with a quenched kinetic energy and its most prominent manifestation is a fractional QHE that has recently been observed in suspended graphene samples.[12,13] Prior indications for strong interactions

stemmed from the high-field QHE at $\nu=0$, which indicates a stronger lifting of the fourfold spin-valley degeneracy of graphene than what one would expect from single-particle effects.[14,15]

Similarly to the $B=0$ case, the Coulomb interaction between electrons in completely filled LLs may be viewed as a weak perturbation because of the energy gap between adjacent LLs. Its role in the dispersion relation and Fermi velocity renormalization of graphene is an open question which has been addressed both theoretically[16–18] and experimentally, in the framework of transmission spectroscopy.[19–23] As compared to the 2DEG with a parabolic band dispersion (as in GaAs/AlGaAs and Si/SiGe heterostructures), the situation is strikingly different in graphene, where the effect of electron-electron interactions may be probed at zero wave vector. Indeed, in the former, LL quantization leads to a set of equidistant LLs separated by the cyclotron frequency. Kohn's theorem states that in these systems, homogeneous electromagnetic radiation can only couple to the center-of-mass coordinate. Therefore internal degrees of freedom associated with the Coulomb interaction cannot be excited by such optical probes.[24] Then, the dispersion relation of spin-conserving magnetoplasmons at zero wave vector is equal to the bare cyclotron energy, irrespective of existing electronic correlations.[25] A similar consideration holds also for spin-wave (SW) modes, for which Larmor's theorem states that the Coulomb interaction does not renormalize the zero-wave-vector dispersion of the spin excitons.[26] However, the dispersion of spin-flip (SF) modes in a 2DEG are shifted from the bare cyclotron resonance even at zero wave vector, due to electron-electron interactions. Therefore, these excitations are the only suitable modes to study the many-body effects in a 2DEG by means of optical measurements.[27–29]

Furthermore, electron-electron interaction in the regime of the integer QHE yield collective excitations that are different from those in the 2DEG, instead of inter-LL excitations with a rather weak wave-vector dispersion, called magnetoexcitons (MEs), one finds linear magnetoplasmons that involve superpositions of different LL transitions.[30,31] Also MEs that may play a role in the vicinity of $q=0$ have been

studied theoretically in graphene and it has been shown that Coulomb interactions yield a renormalization of the transition energy at zero wave vector[16,17,32] that indicates that Kohn's theorem does not apply to graphene. In comparison to these works, here we put more emphasis on spin-changing modes and on the effect of LL mixing.

A convenient way of assessing the magnetic field strength is in terms of four characteristic length scales: the magnetic length l_B, the carbon-carbon distance a, the Fermi wavelength λ_F, and the Thomas-Fermi screening length λ_{TF} $\sim \lambda_F / \alpha_G$, where $\alpha_G \equiv e^2 / \hbar \varepsilon v_F$ measures the relative strength of Coulomb interactions. In practice, the magnetic length is always much larger than the lattice spacing $l_B \gg a$ because the flux per unit cell is much smaller than the flux quantum ($B \ll 40\,000$ T). The weak LL mixing approximation, which we will use when studying the particle-hole excitations, requires $e^2 / (\varepsilon l_B \omega_C) \ll 1$, where ω_C is the cyclotron frequency and corresponds to a strong field such that $l_B \ll \lambda_{TF}$. As in graphene α_G is of order 1, $\lambda_{TF} \sim \lambda_F$ and the weak LL mixing is also the small filling factor limit $l_B \ll \lambda_F$. In the following, we will consider two limits: either a strong magnetic field (meaning $l_B \ll \lambda_F$ or typically $B \gg 20$ T) or a weak magnetic field (meaning $l_B \gg \lambda_F$ or typically $B \ll 20$ T).

In this paper, we study both spin-conserving ME and spin-dependent SF and SW modes in the regime of the integer QHE. Following the scheme introduced by Kallin and Halperin (KH) for the 2DEG,[25] the Coulomb interaction is treated within the framework of the time-dependent Hartree-Fock (TDHF) and strong-field approximation [for which $e^2 / (\varepsilon l_B \omega_C) \ll 1$, which insures that LL mixing is weak], the validity of which is discussed. Indeed, we find that whereas SF and SW may be accounted for correctly in graphene within the KH approximation in the limit of a strong magnetic field and when the Fermi level lies near the $n = 0$ LL, its validity in the treatment of spin-conserving ME is questionable even in these limits. This difference between MEs and SF (and SW) excitations stems from the depolarization term, accounted for in the random-phase approximation (RPA), which is present only in the ME dispersion and which yields a strong LL mixing at nonzero values of the wave vector. This LL mixing eventually leads to the formation of linearly dispersing plasmon-type modes that have been obtained within an RPA treatment of the electronic polarizability in graphene.[30,31]

Finally, we consider the opposite limit of graphene in a weak magnetic field and compute the exchange correction to the chemical potential. We find that the exchange correction to the single-particle dispersion presents the same dependence in the two limits, strong and weak magnetic field, proportional to the square root of the ultraviolet cutoff in the Landau levels. On the other hand, the exchange correction to the particle-hole dispersion diverges logarithmically with the cutoff.

The paper is organized as follows. In Sec. II, we first revisit Kohn's (Sec. II A) and Larmor's (Sec. II B) theorems in the context of graphene and their impact on collective excitations in general. We then study the excitonic modes in graphene in a strong magnetic field, within the KH approximation. In Sec. III we calculate the exchange correction to the chemical potential, in the weak magnetic field limit
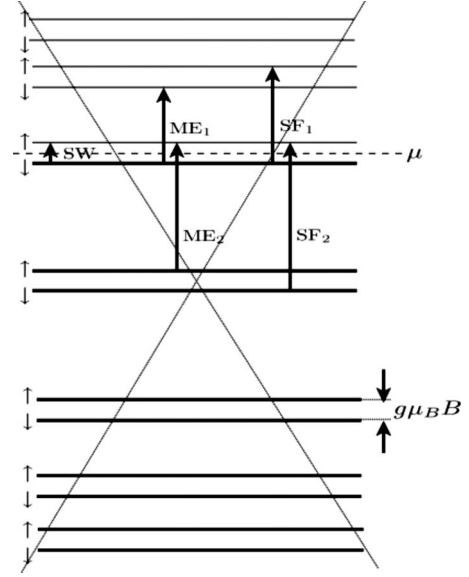

FIG. 1. Sketch of the particle-hole excitations studied in the text. Each Landau level is split in two sublevels, separated by the Zeeman gap, $\Delta E_z = g \mu_B B$. Here, $\uparrow$ indicates $s_z = +1/2$ and $\downarrow$, $s_z = -1/2$. Label ME stands for magnetoexciton (or magnetoplasmon) where the particle and the hole have the same spin. SF denotes the spin-flip excitation, in which the electron and the hole do not only reside in different LLs but also have different spin. Finally, SW denotes the spin-wave mode, which is an intra-LL transition where the electron and the hole have a different spin orientation and where we have taken into account a nonzero Zeeman energy.

and/or for highly doped samples. Our main conclusions are summarized in Sec. IV and the technical details of the calculations are provided in Appendices A and C.

II. EXCITONIC MODES IN GRAPHENE IN THE INTEGER QHE

In spin-flip modes, an electron is both promoted from one LL to the next one and its spin is reversed. They carry a spin $S_z = s_z^e - s_z^h = \pm 1$, where $s_z^{e(h)}$ is the z component of the electron (hole) spin. We use the term magnetoexciton (ME, sometimes also called magnetoplasmon in the literature) to denote spin-conserving excitations, where the electron and the hole reside in different LLs and have the same spin. In SW modes, the two particles have the same LL index but opposite spin. SF modes, MEs and SWs are the basic excitations of a quantum-Hall system with a finite Zeeman splitting, as sketched in Fig. 1.

A. Fate of Kohn's theorem in graphene

Before calculating the dispersion relations of the different excitonic modes, we discuss here qualitatively the expectations for graphene with respect to the 2DEG with a parabolic band dispersion. In the latter, Kohn's theorem[24] states that electromagnetic absorption, irrespective of the strength of the Coulomb interaction, occurs only at the cyclotron frequency $\omega_C = eB / m_b$, in terms of the band mass m_b. Here and in the remainder of this paper, we consider a system of units

with $\hbar \equiv c \equiv 1$. Because this absorption process is associated with an inter-LL transition from the last occupied to the first unoccupied level, it means that the lowest-energy ME must converge to the noninteracting value at zero wave vector. This statement remains valid also for higher harmonics, such that the ME dispersion has $\Omega_{\mathrm{ME}}(q \to 0) \to m\omega_C$, where $m = n_e - n_h$ is the difference between the LL index of the electron (n_e) and that of the hole (n_h).

1. Kohn's theorem in the 2DEG

In order to investigate the fate of Kohn's theorem in graphene, let us recall the main steps in the argument for the 2DEG. In the latter, the Hamiltonian of N noninteracting electrons can be expressed in terms of the gauge-invariant momenta $\boldsymbol{\Pi}_j = \mathbf{p}_j + e\mathbf{A}(\mathbf{r}_j)$, where $\mathbf{r}_j$ and $\mathbf{p}_j$ are the position and its conjugate (gauge-dependent) momentum, respectively, of the jth electron with charge $-e$ (we choose $e > 0$ to be the *positive* elementary charge),

$$H_0 = \frac{1}{2m_b}\sum_{j=1}^{N} \boldsymbol{\Pi}_j^2. \tag{1}$$

From the total gauge-invariant momentum $\boldsymbol{\Pi} = \Sigma_j \boldsymbol{\Pi}_j$, we define the raising and lowering operators $\Pi^{\pm} = \Pi_x \pm i\Pi_y$, which satisfy the commutation relations $[\Pi^{\pm}, H_0] = \mp(1/m_b l_B^2)\Pi^{\pm}$ with the Hamiltonian H_0. This leads to the equation

$$H_0(\Pi^{\pm}|\psi^0\rangle) = (E^0 \pm \omega_C)(\Pi^{\pm}|\psi^0\rangle), \tag{2}$$

which means that the application of $\Pi^{\pm}$ on an (N-particle) eigenstate $|\psi^0\rangle$ (with energy E^0) of H_0 yields another eigenstate with energy $E^0 \pm \omega_C$.

The first observation is that this equation remains valid also in the presence of electron-electron interactions V that commute with the total momentum $[\boldsymbol{\Pi}, V] = 0$, such as the Coulomb interaction, if one replaces the noninteracting state $|\psi^0\rangle$ by an eigenstate $|\psi\rangle$ of the full Hamiltonian $H = H_0 + V$, as well as the energy E^0 by that, E, of the state $|\psi\rangle$.

Second, one notices that the electromagnetic light field with frequency ω couples to the electronic system via the Hamiltonian

$$H_{LM}(t) = \frac{e}{2i\omega}e^{-i\omega t}\mathbf{E}(\omega) \cdot \sum_j \mathbf{v}_j + \text{H.c.}, \tag{3}$$

where $\mathbf{E}(\omega)$ is the electric component of the light field and $\mathbf{v}_j$ the velocity operator of the jth electron. In the 2DEG with a parabolic band dispersion, the velocity operator is readily expressed in terms of the gauge-invariant total momentum, $\Sigma_j \mathbf{v}_j = \boldsymbol{\Pi}/m_b$, such that the light-matter coupling, Eq. (3), is linear in the operators $\Pi^{\pm}$. As mentioned above, this induces then a transition from a state $|\psi\rangle$ with energy E to a state $\Pi^{\pm}|\psi\rangle$ with energy $E \pm \omega_C$, i.e., the only absorption peak for light occurs at the cyclotron frequency ω_C.[24]

2. Difference in graphene

Although also in graphene the total gauge-invariant momentum $\boldsymbol{\Pi}$ commutes with the interaction Hamiltonian V but not with H_0, one first notices that it may no longer be ex-

pressed in terms of the velocity operators of (now relativistic) electrons because of the vanishing band mass. The velocity operator is a 2×2 matrix $\mathbf{v}_j = v_F \boldsymbol{\sigma}_j = v_F(\sigma_j^x, \sigma_j^y)$, in terms of the Pauli matrices σ^x and σ^y, and it is not a conserved quantity even in the absence of interactions. The application of the velocity operator on an eigenstate of the non-interacting Hamiltonian $H_0 = \Sigma_j v_F[\mathbf{p}_j + e\mathbf{A}(\mathbf{r}_j)] \cdot \boldsymbol{\sigma}_j$, for which $[\mathbf{v}_j, H_0] \neq 0$, yields, even in the absence of a magnetic field, spontaneous interband transitions that are at the origin of the so-called *zitterbewegung*.[33] As a consequence, the light-matter coupling Hamiltonian (3), the form of which is also valid for graphene, may no longer be expressed in terms of $\Pi^{\pm}$. Indeed, the velocity operator in Hamiltonian (3) yields transitions involving LLs with adjacent indices n and $n \pm 1$, as in the 2DEG, but the *zitterbewegung* translated to the magnetic field case[34] furthermore yields interband excitations, such that the dipolar selection rules λ_h, $n \to \lambda_e$, $n \pm 1$ are associated with the energies

$$E_{kin}^{(n,\lambda_e,\lambda_h)} = \frac{v_F}{l_B}\sqrt{2}(\lambda_e\sqrt{n+1} - \lambda_h\sqrt{n}), \tag{4}$$

where one expects absorption peaks. Therefore, already in the noninteracting limit, one expects a plethora of absorption peaks, that have indeed been observed experimentally,[19–22] and not a single cyclotron resonance as in the case of the 2DEG with a parabolic dispersion relation.

Furthermore, because the kinetic Hamiltonian (1) becomes $H_0 = v_F \Sigma_j \boldsymbol{\Pi}_j \cdot \boldsymbol{\sigma}_j$ in graphene, one loses the possibility of writing an equation of type (2) for graphene, neither in terms of the total momentum $\boldsymbol{\Pi}$ nor with the help of $\Sigma_j \mathbf{v}_j$, which as we mentioned is not conserved. There is thus no protection of the energies, Eq. (4), when interactions are taken into account. Indeed, the latter renormalize the absorption energies,[16,17,32] as we discuss below, in contrast to the 2DEG, where the absorption energy is protected by Kohn's theorem, and the ME modes no longer converge to the non-interacting inter-LL transition energies

$$E_{kin}^{(n_e,n_h)} = \frac{v_F}{l_B}\sqrt{2}(\lambda_e\sqrt{n_e} - \lambda_h\sqrt{n_h}) \tag{5}$$

in the zero-wave-vector limit.

B. Larmor's theorem applied to graphene

In addition to ME excitations that do not involve the electronic spin, one may investigate spin excitations on rather general grounds. Larmor's theorem states that in the long-wavelength limit, the SW dispersion tends to the (bare) Zeeman splitting, $\Omega_{\mathrm{SW}}(q \to 0) \to g\mu_B B$.[26] This theorem may be understood from the symmetries of the Hamiltonian $H = H_0 + H_{int} + H_Z$. In the absence of the Zeeman term H_Z, the Hamiltonian respects the SU(2) symmetry associated with the electronic spin, i.e., both the total spin operator $\hat{S}_{tot}^2$ and any of the components $\hat{S}_{tot}^{\mu}$, for $\mu = x, y, z$, commute with the Hamiltonian. Since one cannot diagonalize all components of the total spin simultaneously, one needs to choose a particular one, and this is naturally the one chosen by the Zeeman effect (here $\hat{S}_{tot}^z$), such that the full Hamiltonian com-

mutes with $\hat{S}_{tot}^2$ and $\hat{S}_{tot}^z$. The quantum numbers associated with the spin, S and S^z, are therefore good quantum numbers for the full interacting N-particle Hamiltonian, such that all possible states have energies $E = E(S, S^z, \ldots) + g\mu_B B S^z$, where the dots ... represent other quantum numbers that characterize the interacting system. The essence of this expression is that the full interacting N-particle system may be viewed as a large spin that precesses in a magnetic field with the fundamental (Larmor) frequency $\omega_L = g\mu_B B$. Whereas this frequency is affected by the (crystalline) environment via the effective g factor, the latter remains unaltered by the electron-electron interactions. Applied to the present problem of collective excitations, this means that the Zeeman term does not represent a further complication to the SU(2) symmetric Hamiltonian $H_0 + H_{int}$, which thus needs to be diagonalized first.

These rather obvious considerations allow us to understand easily Larmor's theorem if one notices that, in the absence of a Zeeman effect, the SW mode is just the Goldstone mode of a ferromagnetic ground state in which all spins are spontaneously polarized. This ferromagnetic state arises due to exchange-interaction effects when not all subbranches of a particular LL are completely filled.[35] The Goldstone mode is characterized by a dispersion relation that vanishes (as q^2 for a SW mode[36]) in the zero-wave-vector limit, $\omega_G(q \to 0) \to 0$, which means that the different states of the ground-state manifold (i.e., the different polarizations) are connected by a global rotation of zero-energy cost that is precisely the $q=0$ Goldstone mode. In the presence of the Zeeman effect, which chooses a particular orientation of the total spin, one thus obtains a SW mode that tends to the energy $\Omega_{SW}(q \to 0) \to g\mu_B B S_z$, where $S_z = 1$, as stated by Larmor's theorem.

One notices that, in contrast to the above discussion of Kohn's theorem, the (non)relativistic character of H_0 has never played a role in the argument, and Larmor's theorem therefore also applies in the case of graphene. Moreover, one is confronted in graphene with an additional twofold valley degeneracy, that may be taken into account by an SU(2) valley isospin. Although the SU(2) valley symmetry is not respected by the interaction Hamiltonian, the symmetry-breaking terms are strongly suppressed (by a factor of $a/l_B \sim 0.005\sqrt{B}$ [T], in terms of the carbon-carbon distance $a = 0.14$ nm) such that the interaction Hamiltonian is approximately SU(2) valley symmetric.[37,38] Therefore the above arguments apply also to possible valley-ferromagnetic states in graphene, i.e., there are valley-isospin-wave modes that vanish in the $q \to 0$ limit and that may become eventually gapped by a "valley-Zeeman" effect $H_{v\text{-}Z}$ that, if it may be written in terms of components of the total valley isospin, yields a simple energy offset to the dispersion. In the remainder of the paper, we concentrate on collective excitations that involve only the physical spin.

In addition to this generalization of Larmor's theorem to the valley isospin, it may also be generalized to the SF modes, which involve not only different spin states but also different LLs. The dispersion of the collective SF modes may be fully understood from the Hamiltonian $H_0 + H_{int}$, whereas the energy $g\mu_B B S_z$ associated with the Zeeman effect can be simply added at the end of the calculation as a global (wave-

vector-independent) constant. However, as we shall discuss below, the energy of the SF modes does not converge to the simple sum of the Zeeman and the transition energies, Eq. (5), in the zero-wave-vector limit, but they are renormalized by the interaction energy, both in graphene and in the 2DEG.[27]

C. Dispersion relation of the excitonic modes

In graphene, the energies of ME, SW, and SF modes can be expressed as

$$\Omega_{ME}(q) = E_{kin}^{(n_e, n_h)} + \Delta E^{(n_e, s_z^e; n_h, s_z^h)}(q), \tag{6}$$

$$\Omega_{SW}(q) = g\mu_B B S_z + \Delta E^{(n_e, s_z^e; n_h, s_z^h)}(q), \tag{7}$$

$$\Omega_{SF}(q) = E_{kin}^{(n_e, n_h)} + g\mu_B B S_z + \Delta E^{(n_e, s_z^e; n_h, s_z^h)}(q), \tag{8}$$

where S_z is the z component of the exciton spin and $E_{kin}^{(n_e, n_h)}$ is the transition energy in the absence of interactions given by Eq. (5). The contribution $\Delta E^{(n_e, s_z^e; n_h, s_z^h)}$ consists of three terms (see Appendix A for details): a depolarization or exchange term $E_x(q)$, which is accounted for in the RPA approximation, a direct Coulomb interaction between the electron and hole (vertex corrections) $E_v(q)$, and the difference between the exchange self-energy of the electron and that of the hole, $E_{exch} = \Sigma_e - \Sigma_h$. Notice that $E_x(q)$ is only relevant for the ME, because only particles with the same spin can be recombined by means of electron-electron interactions.

It must be kept in mind that, in a 2DEG, the RPA term, which determines the maximum of the ME dispersion at a wave vector $q \sim 1/R_C$ in the TDHF approximation, mixes different LLs, with a mixing amplitude on the order of $e^2/(\varepsilon l_B \omega_C)$.[39] Here $R_C = k_F l_B^2$ is the cyclotron radius, where the Fermi momentum in terms of the index N_F of the topmost fully occupied LL is $k_F = \sqrt{2N_F + 1}/l_B$ for a 2DEG and $k_F = \sqrt{2N_F + \delta_{N_F, 0}}/l_B$ for graphene. This needs to be distinguished from the LL mixing at $q=0$, which determines the stability of the LLs in the presence of electron-electron interactions and which scales as $e^2/\varepsilon R_C \omega_C$. Although the stability of the LLs in graphene is determined by the ratio between the Coulomb energy $e^2/\varepsilon R_C$ and the LL separation $\Delta_n = (\sqrt{2}v_F/l_B)(\sqrt{N_F+1} - \sqrt{N_F}) \sim v_F/R_C$,[38] which happens to be the scale-invariant fine-structure constant $\alpha_G = e^2/\varepsilon v_F$, the situation is again different at the maximum of the ME dispersion at $q \sim 1/R_C$. The order of magnitude of the $q \neq 0$ LL mixing in graphene may be obtained by replacing in $e^2/(\varepsilon l_B \omega_C)$ the 2DEG cyclotron frequency $\omega_C = eB/m_b$ by the density-dependent cyclotron frequency $\omega_C(\mu) = eBv_F^2/\mu$, where $\mu = (v_F/l_B)\sqrt{2N_F}$ is the chemical potential. As a consequence, the validity of the KH approximation fails not only for weak magnetic fields, as in the standard 2DEG, but also at high and intermediate filling factors because the effective cyclotron frequency in graphene decreases as the number of filled LLs increases, leading to an increase in the LL mixing. Therefore, strictly speaking, the results of this section will be valid only in the strong-B limit and for N_F near 0. However, we will see that the KH approximation can still be applied
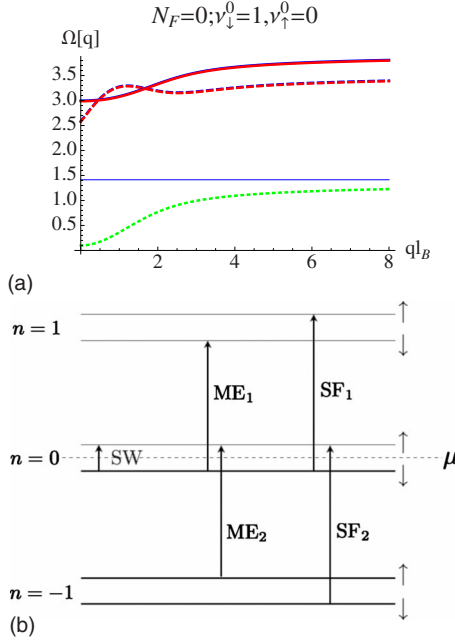
FIG. 2. (Color online) Dispersions (in units of $e^2/\varepsilon l_B$) of the excitonic modes studied for $\nu=0$, i.e., $N_F=0$, $\nu_\downarrow^0=1$, and $\nu_\uparrow^0=0$. SW (dotted green line), $ME_{1,2}$ (dashed blue and red lines, respectively) and $SF_{1,2}$ (solid blue and red lines, respectively) are represented. The thin horizontal line represents the difference in kinetic energy between the electron and the hole $E_{kin}^{(1,0)}$. We have used for the Zeeman term an unphysically large value $g\mu_B B=(1/10)(e^2/\varepsilon l_B)$, for illustration reasons. (b) Schematic representation of the excitonic modes studied. Notice that ME_1 and ME_2 are degenerate in the $N_c \rightarrow \infty$ limit, as well as the SF_1 and SF_2.

for spin-dependent excitations (SW and SF) slightly away from half filling but not to spin-conserving modes (ME). This is a consequence of the absence of the depolarization term $E_x(q)$, which is the main source of LL mixing, in SW and SF modes, whereas it constitutes the main contribution to the dispersion of ME modes.

After these general considerations on collective excitations, we now turn to a discussion of the modes at particular integer filling factors, which are described by

$$\nu = 4N_F - 2 + 2(\nu_\uparrow^{N_F} + \nu_\downarrow^{N_F}), \qquad (9)$$

where N_F is the index of the topmost fully occupied LL, $0 \leq \nu_\sigma^n \leq 1$ is the filling of the spin-σ branch of the nth LL, and the factor of 2 accounts for the twofold valley degeneracy of each spin branch.

D. Modes at filling $\nu=0$

At the charge neutrality point (for a filling factor $\nu=0$), the Fermi level is in the $n=0$ LL (i.e., $N_F=0$), with the spin-$\downarrow$ branch completely filled ($\nu_\downarrow^0=1$) and an empty spin-$\uparrow$ ($\nu_\uparrow^0=0$). The dispersion of the excitonic modes for this situation is shown in Fig. 2(a). The transitions corresponding to the different excitations are schematized in Fig. 2(b). To more easily distinguish between the different modes, we use the notation $\Delta E_{N_F;\nu_\downarrow^{N_F},\nu_\uparrow^{N_F}}(q)$. Therefore, the dispersion of the
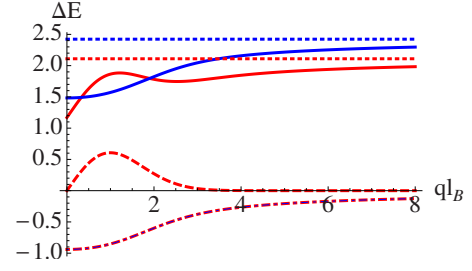

FIG. 3. (Color online) Decomposition of the ME (full red line) and SF (full blue line) mode for $\nu=0$ into the interaction-related components, exchange self-energy (dotted line, red for ME and blue for SF), vertex correction (dashed-dotted line), and RPA term (red dashed line), in units of $e^2/\varepsilon l_B$. The kinetic energy, which yields the same constant offset for both modes, is not taken into account in this decomposition.

magnetoexciton modes $ME_{1,2}$, Eq. (6) will correspond to the kinetic particle-hole energy difference plus a renormalization due to electron-electron interactions, $\Delta E_{0;1,0}^{ME_{1,2}}(q)$, which reads

$$\Delta E^{(1,-1/2;0,-1/2)}(q) = \Sigma_{0;1,0}^{ME_1} + V_{1,0;1,0}^d(q) + 4V_{1,0;1,0}^x(q) \quad \text{for} \quad ME_1$$

and $\Delta E^{(0,+1/2;1,+1/2)}(q) = \Sigma_{0;1,0}^{ME_2} + V_{0,-1;0,-1}^d(q) + 4V_{0,-1;0,-1}^x(q)$ for ME_2, where the expressions for $\Sigma_{0;1,0}^{ME_{1,2}}$ are given in Appendix B. Here $V^x(q)$ are matrix elements of the Hartree term, in which a particle-hole pair recombines, exciting a new particle-hole pair (the usual bubble diagrams). On the other hand, $V^d(q)$ is the Fock term, which accounts for the direct interaction of the excited electron and hole (ladder diagrams). Notice that, due to particle-hole symmetry at this filling, $\Delta E_{0;1,0}^{ME_1}(q) = \Delta E_{0;1,0}^{ME_2}(q)$ and the two modes are degenerate. The first thing one notices is that the dispersion at $q=0$ is shifted with respect to $E_{kin}^{(1,0)}$ [horizontal line in Fig. 2(a)]. This is a consequence of the nonapplicability of Kohn's theorem in graphene, as discussed in Sec. II A, whereas in the 2DEG the theorem is satisfied due to a cancellation between the exchange self-energy and the $q=0$ vertex correction, $E_v(q=0)=-E_{exch}$. Whereas the behavior of the dispersion at short wavelength is dominated by the exchange self-energy and vertex correction terms (see Fig. 3), the peak in the dispersion in the long-wavelength regime is due to the exchange interaction (the RPA term). Furthermore, it is worth pointing out that this contribution rapidly increases as one fills more LLs, as we will see below. This is a direct consequence of the relativistic quantization of the graphene LL spectrum, leading to an important LL mixing at higher fillings and, as a consequence, building an unusual particle-hole excitation spectrum.[30]

This RPA contribution is absent, however, in the SF and SW modes (see Fig. 3). As a consequence, the LL mixing for these modes is less important and makes the KH approximation, as the one applied here, a justified method (especially at strong magnetic fields and for the chemical potential at or near the zero energy LL). The results for these modes are also shown in Fig. 2(a). Electron-electron interactions enter in the dispersion of the former through the term $\Delta E_{0;1,0}^{SF_{1,2}}(q)$, which again due to particle-hole symmetry leads to degenerate modes with contributions $\Delta E^{(1,+1/2;0,-1/2)}(q)=\Sigma_{0;1,0}^{SF_1} + V_{1,0;1,0}^d(q)$ and $\Delta E^{(-1,-1/2;0,+1/2)}(q)=\Sigma_{0;1,0}^{SF_2} + V_{0,-1;0,-1}^d(q)$, re-
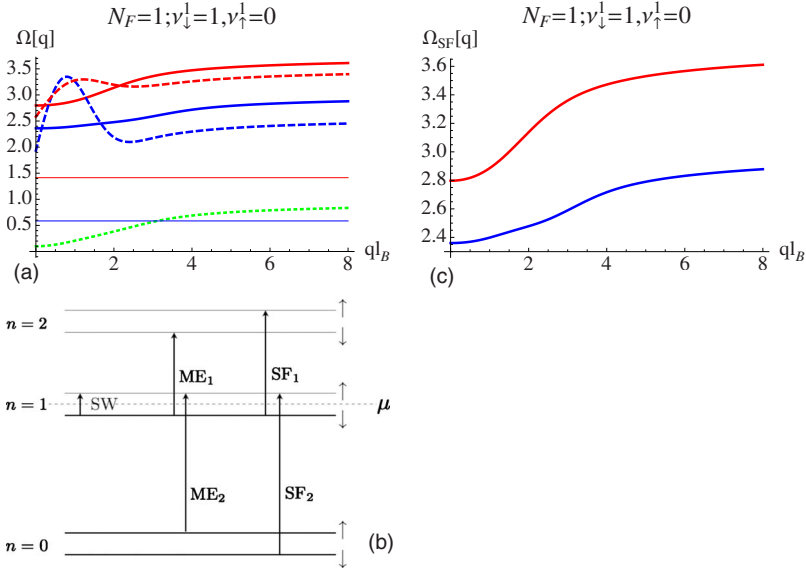
FIG. 4. (Color online) (a) Same as Fig. 2 but for $\nu=4$, with $N_F=1$, $\nu_\downarrow^1=1$ and $\nu_\uparrow^1=0$. ME$_{1,2}$ (dashed blue and red lines, respectively) and SF$_{1,2}$ (solid blue and red lines, respectively) are represented. The thin horizontal lines represent the difference in kinetic energy between the electron and the hole $E_{kin}^{(1,0)}$ and $E_{kin}^{(2,1)}$. (b) Schematic representation of the excitonic modes studied. The degeneracy that occurs at $N_F=0$ is completely lifted at this filling for both, ME and SF modes. For clarity, we show in (c) the SF modes separately.

spectively. As in the 2DEG, the $q\to 0$ limit of the dispersion of these modes is renormalized from the noninteracting value, $E_{kin}^{(n_e,n_h)}+g\mu_B B S_z$. This makes possible the study of correlation effects by optical measurements.

On the other hand, Larmor's theorem still applies in graphene, as one may see from the dispersion of the SW mode. This mode has a $q=0$ dispersion equal to the Zeeman splitting $g\mu_B B S_z$, and a contribution due to electron-electron interaction $\Delta E^{(0,+1/2;0,-1/2)}(q)=\Sigma_{0;1,0}^{SW}+V_{0,0;0,0}^d(q)$, which is finite only at nonzero wave vectors. This implies that, as in the 2DEG, the g factor is not influenced by the Coulomb interaction. The SW disappears if we fill the next LL, for $\nu=2$, with $N_F=0$, $\nu_\downarrow^0=1$, and $\nu_\uparrow^0=1$. The dispersions of the ME and SF modes (not shown here) are similar to the previous case with the difference that the degeneracy of the latter is lifted, but only by a constant term equal to the double of the Zeeman energy, in agreement with the arguments of Sec. II B.

E. Modes at filling $\nu=4$

The relativistic nature of the LLs in graphene is clearly visible if we go beyond $N_F=0$, as shown in Fig. 4(b) for a filling factor of $\nu=4$, with $N_F=1$, $\nu_\downarrow^1=1$, and $\nu_\uparrow^1=0$. At this filling, the nonequidistancy of the LLs lifts the degeneracy of the two ME modes, as well as the two SF modes. In addition, the exchange contribution to the ME modes, which leads to the peak in their dispersion, increases as we decrease the separation between the LLs of the electron and the hole. This yields a strong mixing among the different branches of MEs, as may be seen in Fig. 4(a). In fact, the height of the peak associated with the ME$_1$ [with $n_e=2$ and $n_h=1$, as represented in Fig. 4(b)], is larger than that of ME$_2$ (with $n_e=1$ and $n_h=0$). This is due to the linear dispersion of the spectrum, which enhances the quantum effects as we go to higher filling factors. Taking into account that we are showing here only two of the spin-conserving excitations possible for this filling (the ones involving the more adjacent LLs to the chemical potential), one can conclude that no *single* MEs will be accessible experimentally at finite wave vectors, but a

superposition of them. Therefore, the TDHF method in the strong-field approximation is not valid for the spin-conserving modes, and the inclusion of a much higher number of modes is necessary to obtain a reliable result. In fact, this overlap of different MEs leads to a new set of collective modes, the linear magnetoplasmons, which have been studied elsewhere.[30]

Notice that the above arguments are valid only at nonzero values of the wave vector, whereas the LL mixing effects are less pronounced at $q=0$, which is the relevant ME energy in magneto-optical experiments.[19–22] However, as we have mentioned above, also at $q=0$ the ME energy, which is the inter-LL transition energy measured in spectroscopy, is renormalized due to electron-electron interactions.

The mixing between different contributions is less dramatic for the SF modes, as one sees in Fig. 4(c), where we show a plot with only the SF modes at this filling. One notices how the two modes are clearly decoupled, making the use of the KH approximation more justified, because of the absence of the RPA term which is responsible, in the ME case, for the LL mixing at nonzero values of the wave vector. Although not too clearly, it is appreciable that the number of relative extrema (maxima and minima) in the dispersion of SF$_1$ (blue line) is higher than for SF$_2$ (red line). This is directly related to the node structure of the (hole) LL wave function.[31] These maxima and minima lead to hot spots in the dispersion that may be detected by Raman spectroscopy techniques.[40]

III. RENORMALIZATION OF THE CHEMICAL POTENTIAL

To gain further insight into the effect of electronic interactions in a graphene flake, we calculate in this section the exchange correction to the chemical potential, from a density-matrix approach. This is the first step toward including electron-electron interaction in the system. The correction is intrinsically related to the antisymmetry of the electronic wave function, which implies, even in the absence of

interactions, a certain amount of correlation between the positions of two particles with the same spin. Furthermore, its sign is always negative, due to the fact that it is the interaction of each electron with the positive charge of its exchange hole. One of the effects of Coulomb interaction is a renormalization of the chemical potential μ, which at zero temperature is the partial derivative of the total energy with respect to the number of particles. It contains a contribution from the kinetic energy and also from interactions. The latter can be written as a mean-field contribution plus correlation: $\mu = K + \mu^{ex} + \mu^c$, where K is the kinetic energy, and μ^{ex} and μ^c are the exchange and correlation corrections to the chemical potential, respectively. As usual, the direct (Hartree) mean-field contribution does not appear as it is compensated by the positively charged background (or neutralizing background), see the jellium model. Furthermore, the exchange interaction can lead to a ferromagnetic instability in a dilute electron gas.[39] In graphene, ferromagnetism due to the exchange interaction between Dirac fermions has also been studied.[41] In a magnetic field, μ^{ex} can be obtained from the pair correlation function $g(r)$ (see Appendix C for details of the calculation) as

$$\mu^{ex} = \bar{n} \int d^2\mathbf{r} \frac{e^2}{\varepsilon r} [g(r) - 1], \tag{10}$$

where $\bar{n} = 4(1 + N_c + N_F)/(2\pi l_B^2)$ is the electron density for graphene in a magnetic field. N_F is the index of the last occupied LL, related to the filling factor by $\nu = 4N_F + 2$, and N_c is a cutoff chosen such that $(4N_c + 2)N_B = 2N_{u.c.}$, where $N_B = \mathcal{A}/2\pi l_B^2$ is the degeneracy of each LL, $\mathcal{A}$ is the surface of the sample, $N_{u.c.}$ is the number of occupied unit cells in the system, the factor 2 is due to spin degeneracy, and $4N_c + 2$ is the number of filled sublevels of the valence band for undoped graphene. N_c is the index of the last LL in the band (a kind of bandwidth) and is roughly given by $N_c \approx N_{u.c.}/(2N_B) = 2\pi l_B^2/(3\sqrt{3}a^2) \approx 40\,000/B$ [T] which is always much greater than 1 in practice. The fact that $N_c \gg 1$ is just the statement that, with available magnetic fields, the flux per unit cell is always much smaller than the flux quantum. In this respect, we are always in the weak-field limit. An exact solution of Eq. (10) is possible in the limit N_c, $N_F \gg 1$, as shown in Eq. (C8). This correction would eventually involve a renormalization of N_F, this is, a shift of the chemical potential as compared to the noninteracting case.

Notice that, contrary to the strong magnetic field assumption done in the previous section, this is the opposite case, namely the weak magnetic field limit. The strong field limit is actually the KH approximation of weak LL mixing.[25] As stated in Sec. II C, the criterion for a weak LL mixing is $e^2/(\varepsilon l_B \omega_c) \ll 1$. In graphene, because the fine structure constant $\alpha_G = e^2/\varepsilon v_F$ is of order 1, it means that $k_F l_B \ll 1$, which means $N_F \approx 0$ (i.e., $N_F \ll 1$) or in other words $B \gg 20$ T. This is the assumption made in the previous section, whereas in this section we assume the opposite limit ($B \ll 20$ T or $N_F \gg 1$). In a standard 2DEG with a parabolic band, the weak magnetic field limit implies that the typical Coulomb energy exceeds the cyclotron frequency ω_C. This allows us to start

from the Landau Fermi-liquid theory at zero magnetic field.[42] In the case of graphene, this limit is even more relevant due to the relativistic quantization of the spectrum into nonequidistant LLs, the relative separation of which decreases as the energy increases. Therefore, even in a strong magnetic field, the strength of the Coulomb interaction can be much higher than the separation between the LLs adjacent to the chemical potential (the effective cyclotron frequency in graphene) if the system is sufficiently doped. Further simplification is possible if $1 \ll N_F \ll N_c$. In this limit we obtain (see Appendix C) that the exchange correction to the Fermi energy behaves asymptotically as

$$\mu^{ex} \simeq -\frac{e^2}{\varepsilon l_B} \frac{16\sqrt{2}}{3\pi} \sqrt{N_c}. \tag{11}$$

This contribution is expected since the energy calculated above includes the interaction energy of the vacuum of negative energy particles. It is interesting to compare this leading behavior of the exchange energy, valid for high filling factors, to the exchange self-energy obtained in Appendix B valid at low fillings [see, e.g., Eqs. (B8)–(B10) for $N_F = 0$ and 1, respectively]. In the two cases we obtain the same $\sim N_c^{1/2}$ leading behavior.[43] Furthermore, our results agree with the exchange contribution calculated for graphene at zero magnetic field, where a $\Sigma^{ex} \sim -e^2 k_c/\varepsilon$ contribution was found, $k_c \sim 1/a$ being an UV cutoff in momenta.[44] Taking into account that $N_c \sim (l_B/a)^2$, our results for graphene in a magnetic field qualitatively agree with those at $B = 0$. Notice that whereas μ^{ex} diverges as $N_c^{1/2}$ for the single-particle dispersion, the dispersion of a particle-hole pair diverges only logarithmically, because the terms proportional to the square root of N_c for each particle cancel each other, leading to a behavior $E_{exch} \propto \log N_c$. This divergence can be reabsorbed into a renormalization of the Fermi velocity,[7] and its effect for cyclotron resonance measurements has been studied in detail by Shizuya.[32] This renormalization of the chemical potential due to Coulomb interaction should affect the scanning single-electron transistor measurements of compressibility in graphene.[45]

IV. SUMMARY AND CONCLUSIONS

In conclusion, we have studied the SF, SW, and ME (or magnetoplasmon) modes in graphene in the integer QHE regime, in the Kallin-Halperin approximation. The ME dispersion in a 2DEG is not renormalized in the long-wavelength limit due to Kohn's theorem for systems with a parabolic band and Galilean invariance. As a consequence, the correction due to the direct interaction between the electron and the hole is neutralized by their difference in exchange self-energy, $E_v(q=0) = -E_{exch}$, leading to a dispersion that tends to $m\omega_C$ at zero wave vector.[27] In graphene, Kohn's theorem does not apply and the dispersion of the ME modes is renormalized due to many-body effects even at $\mathbf{q} = 0$.

On the other hand, virtual transitions from the vacuum (valence band) enhance the depolarization term of the spin-conserving ME dispersion, which enters through the RPA contribution and which leads to an important LL mixing. We

have shown that the mixing is higher as we increase the LL filling and/or decrease the magnetic field, invalidating the applicability of KH approximation for $\nu \geq 2$, which needs to be restricted to the large-field $N_F = 0$ case.[16,17] One of our main conclusions is that, for ME modes, methods involving more inter-LL transitions than only one need to be considered in the calculation of the spin-conserving collective excitations. This superposition of several inter-LL transitions is at the origin of the strongly dispersing linear magnetoplasmons, which have been obtained within an RPA treatment of the electron-electron interactions.[30,31]

In contrast to the spin-conserving ME modes, the depolarization term is absent in collective excitations where the particle and hole components have opposite spin, and the amount of mixing is less important. Therefore the KH approximation can still be used for these modes in undoped or slightly doped graphene in a strong magnetic field. In a 2DEG, the zero-wave-vector limit of the KH correction of SF modes has a finite contribution, because $E_\nu(q=0) = -(1/2)E_{exch}$ in this case. In graphene, the dispersion of these modes is also renormalized at zero wave vector and leads to a correction that could be detected in inelastic light scattering experiments, by using the same techniques as for a 2DEG.[27–29,40] In contrast to Kohn's theorem, we have shown that Larmor's theorem applies to graphene so that the $q \rightarrow 0$ limit of the SW dispersion is equal to the Zeeman splitting and the g factor is independent of many-body interaction, as in a standard 2DEG.[26] In addition, the g factor is also only weakly affected by band effects in graphene: the effective g factor was measured to be close to its bare value of 2, see Ref. 14.

Finally, we have calculated the exchange shift of the chemical potential in the weak magnetic field limit. We have found that, as for strong magnetic fields, the exchange correction to the chemical potential diverges with the ultraviolet cutoff as $\sim N_c^{1/2}$. However, when the dispersion of an electron-hole pair is considered, the correction associated with the difference in exchange self-energy between the particle and the hole, diverges only logarithmically. This correction leads to a renormalization of the Fermi velocity that seems to explain some recent experimental results.[20–22]

ACKNOWLEDGMENTS

APPENDIX A: POLES OF THE RESPONSE FUNCTION IN THE TIME-DEPENDENT HARTREE-FOCK AND STRONG FIELD APPROXIMATIONS

Within the TDHF approximation, the dispersion relation of the excitonic modes is defined by the poles of the response function, which are solutions to the eigenvector equation [see, e.g., Ref. 46 for the 2DEG],

$$\sum_{\gamma,\delta} \{ \delta_{\alpha,\gamma}\delta_{\beta,\delta}[D(\omega)]^{-1}_{\alpha\beta} - \delta_{s^z_\alpha,s^z_\gamma}\delta_{s^z_\delta,s^z_\beta}V^d_{\alpha,\delta;\beta,\gamma}(\mathbf{q})$$

$$+ \delta_{s^z_\alpha,s^z_\beta}\delta_{s^z_\delta,s^z_\gamma}V^x_{\alpha,\delta;\gamma,\beta}(\mathbf{q})\}B_{\gamma\delta}(\mathbf{q}) = 0, \qquad (A1)$$

where $B_{\gamma\delta}(\mathbf{q})$ are the basis states, and $\alpha \equiv (\lambda_\alpha, n_\alpha, s^z_\alpha)$ labels a

particle with band index λ_α, LL n_α, and s^z_α is the z component of its spin. The sum in Eq. (A1) is restricted, in the strong-field approximation [i.e., weak LL mixing $e^2/(\varepsilon l_B \omega_C) \ll 1$], to pairs of indices such that $n_\gamma - n_\delta = n_\alpha - n_\beta = m$ and $s^z_\gamma - s^z_\delta = s^z_\alpha - s^z_\beta = S^z$. This is what we call the Kallin-Halperin approximation. The matrix elements of the two-particle propagator are

$$D_{\alpha,\beta}(\omega) = \frac{f_\alpha(1-f_\beta)}{\omega - E^{(n_\beta,n_\alpha)}_{kin} - g\mu_B B(s^z_\beta - s^z_\alpha) - E^{exch}_{\beta\alpha} + i\delta}$$

$$- \frac{f_\beta(1-f_\alpha)}{\omega - E^{(n_\beta,n_\alpha)}_{kin} - g\mu_B B(s^z_\beta - s^z_\alpha) - E^{exch}_{\beta\alpha} - i\delta},$$

where $f_\alpha \equiv \Theta(\mu - \lambda_\alpha v_F l_B^{-1}\sqrt{2n_\alpha})$, $\Theta(x)$ being the step function, and $\delta \rightarrow 0^+$. The difference in exchange self-energy between the electron and the hole reads

$$E^{exch}_{\beta\alpha} = \Sigma^\beta - \Sigma^\alpha = \sum_\gamma f_\gamma [\delta_{s^z_\beta,s^z_\gamma}V^d_{\beta,\beta;\gamma,\gamma}(0) - \delta_{s^z_\alpha,s^z_\gamma}V^d_{\alpha,\alpha;\gamma,\gamma}(0)],$$

where the direct term is[16]

$$V^d_{\alpha,\beta;\alpha'\beta'}(\mathbf{q}) = -\frac{1}{4}(\sqrt{2})^{d_{\alpha,\beta;\alpha',\beta'}} \sum_{\mu,\nu=0}^{1} b_\mu(\lambda_\alpha)$$

$$\times b_\nu(\lambda_\beta)b_\mu(\lambda_{\alpha'})b_\nu(\lambda_{\beta'})$$

$$\times \tilde{u}_{c_\mu(\alpha),c_\nu(\beta);c_\mu(\alpha'),c_\nu(\beta')}(\mathbf{q}), \qquad (A2)$$

where $d_{\alpha,\beta;\alpha',\beta'} = \delta_{n_\alpha,0} + \delta_{n_\beta,0} + \delta_{n_{\alpha'},0} + \delta_{n_{\beta'},0}$, $b_0(\lambda) = 1$, $b_1(\lambda) = \lambda$, $c_0(\alpha) = |n_\alpha|$, and $c_1(\alpha) = |n_\alpha| - 1$, and

$$\tilde{u}_{\alpha,\beta;\alpha'\beta'}(\mathbf{q}) = \frac{1}{l_B^2}\int d\mathbf{r} v(\mathbf{r} - l_B^2\hat{\mathbf{u}}_z \times \mathbf{q})\mathcal{F}^*_{\alpha',\beta'}(\mathbf{r})\mathcal{F}_{\alpha,\beta}(\mathbf{r}),$$

$$(A3)$$

$v(\mathbf{r}) = e^2/\varepsilon r$ being the Coulomb potential and

$$\mathcal{F}_{\alpha,\beta}(\mathbf{r}) = \frac{1}{\sqrt{2\pi}}\frac{1}{2^{|m|/2}}\frac{n_<!}{\sqrt{n_\alpha!n_\beta!}}e^{-im\phi}\,\text{sgn}(m)^m$$

$$\times \left(\frac{r}{l_B}\right)^{|m|}L^{|m|}_{n_<}\left(\frac{r^2}{2l_B^2}\right)e^{-r^2/4l_B^2}, \qquad (A4)$$

where $n_< = \min(n_\alpha, n_\beta)$, $m = n_\alpha - n_\beta$, and $e^{i\phi} = (x+iy)/|x+iy|$, and $\text{sgn}(m)^m = 1$ for $m = 0$. The exchange matrix elements read

$$V^x_{\alpha,\beta;\alpha'\beta'}(\mathbf{q}) = -\frac{1}{4}(\sqrt{2})^{d_{\alpha,\beta;\alpha',\beta'}}$$

$$\times \sum_{\mu,\nu=0}^{1} b_\mu(\lambda_\alpha)b_\nu(\lambda_\beta)b_\mu(\lambda_{\alpha'})b_\nu(\lambda_{\beta'})$$

$$\times \tilde{v}_{c_\mu(\alpha),c_\nu(\beta);c_\mu(\alpha'),c_\nu(\beta')}(\mathbf{q}), \qquad (A5)$$

where

$$\tilde{v}_{\alpha,\beta;\alpha'\beta'}(\mathbf{q}) = \frac{1}{l_B^2}\frac{2\pi e^2}{\varepsilon q}\mathcal{F}^*_{\alpha',\beta'}(l_B^2\hat{\mathbf{u}}_z \times \mathbf{q})\mathcal{F}_{\alpha,\beta}(l_B^2\hat{\mathbf{u}}_z \times \mathbf{q}).$$

$$(A6)$$

APPENDIX B: EXCHANGE SELF-ENERGY CONTRIBUTIONS

In this appendix we give analytical expressions for the contributions to ΔE associated to the difference in exchange self-energy between the electron and the hole. For $N_F = 0$; $\nu_\downarrow^0 = 1$, $\nu_\uparrow^0 = 0$, using the notation $\Sigma_{N_F; \nu_\downarrow^{N_F}, \nu_\uparrow^{N_F}}$, we obtain

$$\Sigma_{0;1,0}^{ME_1} = \frac{e^2}{\varepsilon l_B} \left[\frac{3}{4} \sqrt{\frac{\pi}{2}} + \sum_{n=1}^{N_c} \frac{(4\sqrt{n} - 3)\Gamma\left(n - \frac{1}{2}\right)}{16\sqrt{2}\,\Gamma(n+1)} \right] \quad (B1)$$

for ME_1 and

$$\Sigma_{0;1,0}^{ME_2} = \frac{e^2}{\varepsilon l_B} \sum_{n=1}^{N_c} \frac{(4\sqrt{n} + 3)\Gamma\left(n - \frac{1}{2}\right)}{16\sqrt{2}\,\Gamma(n+1)} \quad (B2)$$

for ME_2, where N_c is a high-energy cutoff. Notice that $\Sigma_{0;1,0}^{ME_1} = \Sigma_{0;1,0}^{ME_2}$ in the limit $N_c \to \infty$. The contributions to the spin-flip modes are

$$\begin{aligned}
\Sigma_{0;1,0}^{SF_1} &= \Sigma_{0;1,0}^{ME_1} - V_{1,1;0,0}^d(0) \\
&= \frac{e^2}{\varepsilon l_B} \left[\sqrt{\frac{\pi}{2}} + \sum_{n=1}^{N_c} \frac{(4\sqrt{n} - 3)\Gamma\left(n - \frac{1}{2}\right)}{16\sqrt{2}\,\Gamma(n+1)} \right]
\end{aligned} \quad (B3)$$

for SF_1 and

$$\begin{aligned}
\Sigma_{0;1,0}^{SF_2} &= \Sigma_{0;1,0}^{ME_2} - V_{-1,-1;0,0}^d(0) \\
&= \frac{e^2}{\varepsilon l_B} \left[\frac{1}{4}\sqrt{\frac{\pi}{2}} \sum_{n=1}^{N_c} \frac{(4\sqrt{n} + 3)\Gamma\left(n - \frac{1}{2}\right)}{16\sqrt{2}\,\Gamma(n+1)} \right]
\end{aligned} \quad (B4)$$

for SF_2. Again, $\Sigma_{0;1,0}^{SF_1} = \Sigma_{0;1,0}^{SF_2}$ as the cutoff N_c tends to infinity. On the other hand, the contribution for the SW mode is $\Sigma_{0;1,0}^{SW} = e^2/(\varepsilon l_B)\sqrt{\pi/2}$, which is cut-off independent. The contributions for $N_F = 0$; $\nu_\downarrow^0 = 1$, $\nu_\uparrow^0 = 1$ can be expressed in terms of the previously given $\Sigma_{0;1,0}^{ME_{1,2}}$, as $\Sigma_{0;1,1}^{ME_1} = \Sigma_{0;1,1}^{ME_2} = \Sigma_{0;1,0}^{ME_1}$ for the ME modes and $\Sigma_{0;1,1}^{SF_1} = \Sigma_{0;1,1}^{SF_2} = \Sigma_{0;1,0}^{ME_1}$ for the SF modes.

Finally, the contributions for $N_F = 1$; $\nu_\downarrow^1 = 1$, $\nu_\uparrow^1 = 0$, shown in Fig. 4, are

$$\begin{aligned}
\Sigma_{1;1,0}^{ME_1} = \frac{e^2}{\varepsilon l_B} \Bigg[&\frac{1}{128}(37\sqrt{2} - 8)\sqrt{\pi} \\
&+ \sum_{n=1}^{N_c} \frac{[8\sqrt{n}(4n - 2\sqrt{n} - 3) + 3]\Gamma\left(n - \frac{3}{2}\right)}{128\sqrt{2}\,\Gamma(n+1)} \Bigg]
\end{aligned} \quad (B5)$$

for the ME_1 mode, whereas $\Sigma_{1;1,0}^{ME_2} = \Sigma_{0;1,0}^{ME_1}$ as given in Eq. (B1). For the spin-flip modes we have

$$\Sigma_{1;1,0}^{SF_1} = \frac{e^2}{\varepsilon l_B} \left[\frac{3}{4}\sqrt{\frac{\pi}{2}} + \sum_{n=1}^{N_c} \frac{8\sqrt{n}(4n - 2\sqrt{n} - 3) + 3}{128\sqrt{2}} \frac{\Gamma\left(n - \frac{3}{2}\right)}{\Gamma(n+1)} \right] \quad (B6)$$

for SF_1 while the contribution associated to the second mode is $\Sigma_{1;1,0}^{SF_2} = \Sigma_{0;1,0}^{SF_1}$ and coincides with Eq. (B3). Finally, the N_c-independent contribution to the SW mode is $\Sigma_{1;1,0}^{SW} = \frac{e^2}{\varepsilon l_B}\frac{11}{16}\sqrt{\frac{\pi}{2}}$.

In the following, we calculate the exchange energy of the system at low fillings. First, one notices that the exchange self-energy for undoped graphene ($N_F = 0$; $\nu_\downarrow^0 = 1$, $\nu_\uparrow^0 = 0$) [and similarly for the filling ($N_F = -1$; $\nu_\downarrow^{-1} = 1$, $\nu_\uparrow^{-1} = 1$)] can be calculated as

$$\begin{aligned}
\Sigma^{ex} &= \Sigma_{n=-N_c}^{-1} V_{0,0;n,n}^d(0) \\
&= -e^2/(2\sqrt{2}\varepsilon l_B)\Sigma_{n=1}^{N_c}\Gamma\left(n + \tfrac{1}{2}\right)/\Gamma(n+1),
\end{aligned}$$

which can be summed up exactly to give

$$\Sigma^{ex} = -\frac{e^2}{\varepsilon l_B}\frac{1}{2\sqrt{2}} \left[-\sqrt{\pi} + 2\frac{\Gamma\left(N_c + \frac{3}{2}\right)}{\Gamma(N_c + 1)} \right]. \quad (B7)$$

For $N_c \gg 1$ we obtain the asymptotic behavior

$$\Sigma^{ex} \simeq -\frac{e^2}{\varepsilon l_B}\frac{1}{2\sqrt{2}} \left[-\sqrt{\pi} + 2\sqrt{N_c} + O\left(\frac{1}{N_c}\right)^{1/2} \right] \quad (B8)$$

It is useful to express this result by substituting $\sqrt{N_c}$ by its magnetic field dependence $\sqrt{N_c} \sim l_B/a$. By doing so, we obtain

$$\Sigma^{ex} = -\frac{e^2}{\varepsilon a} \left[\# + \#\frac{a}{l_B} + O\left(\frac{a}{l_B}\right)^2 \right], \quad (B9)$$

where $\#$ stands for some numerical prefactor and $a/l_B = 0.006\sqrt{B}$ [T]. We clearly see that the dominant term, as in Eq. (11), is magnetic field independent.

A similar result is obtained for doped graphene up to the first LL of the conduction band. If ($N_F = 1$; $\nu_\downarrow^1 = 1$, $\nu_\uparrow^1 = 0$) or ($N_F = 0$; $\nu_\downarrow^0 = 1$, $\nu_\uparrow^0 = 1$), then Σ^{ex} is computed as

$$\begin{aligned}
\Sigma^{ex} = \sum_{n=-N_c}^{0} V_{1,1;n,n}^d(0) &= V_{1,1;n,n}^d(0) \\
&+ \frac{e^2}{\varepsilon l_B}\sum_{n=1}^{N_c} \frac{1 + 4\sqrt{n} - 8n}{16\sqrt{2}}\frac{\Gamma\left(n - \frac{1}{2}\right)}{\Gamma(n+1)}.
\end{aligned}$$

Taking $N_c \gg 1$ we obtain the limiting result

$$\begin{aligned}
\Sigma^{ex} \simeq -\frac{e^2}{\varepsilon l_B} \\
\times \left[\frac{1}{8}\sqrt{\frac{\pi}{2}} + \frac{1}{\sqrt{2}}\sqrt{N_c} - \frac{4}{16\sqrt{2}}(1.0646 + \gamma + \ln N_c) \right],
\end{aligned} \quad (B10)$$

where γ is the Euler constant and we have approximated

$\sum_{n=1}^{N_c}(\sqrt{n}\Gamma(n-1/2)/n!-n^{-1})\simeq 1.0646$. Equation (B10) could be accordingly expressed in the form of Eq. (B9) and the result would be the similar as before: the leading term in the exchange contribution to the chemical potential does not depend on the magnetic field.

APPENDIX C: CORRELATION FUNCTION

The one-particle density matrix for the K valley (labeled here by +) can be defined as $\rho_+(\mathbf{r},\mathbf{r}')=\Sigma_\sigma\Sigma_{\lambda,n}\rho_{+,\lambda,n}(\mathbf{r},\mathbf{r}')$ in terms of the density matrix of the nth LL of the λ band of the K valley $\rho_{+,\lambda,n}(\mathbf{r},\mathbf{r}')=\Sigma_k\Psi_{\lambda nk}^{+\dagger}(\mathbf{r})\Psi_{\lambda nk}^{+}(\mathbf{r}')$, where $\Psi_{\lambda nk}^{+}(\mathbf{r})$ are the K-valley LL wave function. The wave function for graphene in a magnetic field can be constructed from the corresponding nonrelativistic LL wave functions of a 2DEG with a parabolic band dispersion. In the Landau gauge, where the vector potential is $\vec{A}=(0,Bx,0)$, they can be written as

$$\Psi_{nk}^{+}(\mathbf{r})=\frac{1}{\sqrt{L}}e^{-iky}\begin{pmatrix}-i\lambda 1_n^*\phi_{n-1,k}(x)\\2_n^*\phi_{n,k}(x)\\0\\0\end{pmatrix} \quad \text{(C1)}$$

for the K (+) valley and

$$\Psi_{nk}^{-}(\mathbf{r})=\frac{1}{\sqrt{L}}e^{-iky}\begin{pmatrix}0\\0\\2_n^*\phi_{n,k}(x)\\-i\lambda 1_n^*\phi_{n-1,k}(x)\end{pmatrix} \quad \text{(C2)}$$

for the K' (−) valley, where

$$\phi_{n,k}(x)=\frac{1}{\sqrt{2^n n!}\sqrt{\pi}l_B}e^{-z^2/2}H_n(z). \quad \text{(C3)}$$

In the previous expression $z=x-kl_B^2/l_B$ and H_n are Hermite polynomial, and we have defined $1_n^*=\sqrt{(1-\delta_{n,0})/2}$ and $2_n^*=\sqrt{(1+\delta_{n,0})/2}$. One obtains therefore

$$\rho_{+,\lambda,n}(\mathbf{r},\mathbf{r}')=\frac{1}{2\pi l_B^2}e^{-i(y-y')(x+x')/2l_B^2}e^{-|\mathbf{r}-\mathbf{r}'|^2/4l_B^2}$$
$$\times\left[1_n^{*2}L_{n-1}\left(\frac{|\mathbf{r}-\mathbf{r}'|^2}{2l_B^2}\right)+2_n^{*2}L_n\left(\frac{|\mathbf{r}-\mathbf{r}'|^2}{2l_B^2}\right)\right].$$

The sum $\Sigma_{\lambda,n}\rho_{+,\lambda,n}(\mathbf{r},\mathbf{r}')$ in the band and LL indices is decomposed into an interband and an intraband contributions,

$$\sum_{n=1}^{N_c}\rho_{+,\lambda=-1,n}(\mathbf{r},\mathbf{r}')+\sum_{n=1}^{N_F}\rho_{+,\lambda=+1,n}(\mathbf{r},\mathbf{r}'). \quad \text{(C4)}$$

Furthermore, it can be checked that $\sum_{n=1}^{N_0}1_n^{*2}L_{n-1}^0(x)=(1/2)L_{N_0-1}^1(x)$ and $\sum_{n=1}^{N_0}2_n^{*2}L_n^0(x)=(1/2)L_{N_0}^1(x)$, where N_0

$=N_c,N_F$. Therefore, neglecting the Zeeman splitting, we obtain for the K-valley one-particle density matrix,

$$\rho_+(\mathbf{r},\mathbf{r}')=\frac{1}{2\pi l_B^2}e^{-i(y-y')(x+x')/2l_B^2}e^{-|\mathbf{r}-\mathbf{r}'|^2/4l_B^2}\left[L_{N_c-1}^1\left(\frac{|\mathbf{r}-\mathbf{r}'|^2}{2l_B^2}\right)\right.$$
$$\left.+L_{N_c}^1\left(\frac{|\mathbf{r}-\mathbf{r}'|^2}{2l_B^2}\right)+(N_c\rightarrow N_F)\right], \quad \text{(C5)}$$

where $(N_c\rightarrow N_F)$ indicates the replacement of N_c by N_F. Considering the K'-valley contribution, the one-particle density matrix is obtained as $\rho(\mathbf{r},\mathbf{r}')=2\rho_+(\mathbf{r},\mathbf{r}')$. From this, one can obtain the pair-correlation function $g(\mathbf{r},\mathbf{r}')$, which is defined as the normalized probability of finding an electron at position $\mathbf{r}$ given that, at the same time, there is another electron at position $\mathbf{r}'$. It can be expressed in terms of the density matrix as[39] $g(\mathbf{r},\mathbf{r}')=1-|\rho(\mathbf{r},\mathbf{r}')|^2/[n(\mathbf{r})n(\mathbf{r}')]$, where $n(\mathbf{r})\equiv\rho(\mathbf{r},\mathbf{r})=4(1+N_c+N_F)/(2\pi l_B^2)$ is the electron density and we have used the fact that $L_n^\alpha(0)=(n+\alpha)!/(n!\alpha!)$. Setting $\mathbf{r}'=0$ we find

$$g(r)=1-\frac{1}{N^2}\left\{2e^{-r^2/4l_B^2}\left[1+L_{N_c-1}^1\left(\frac{r^2}{2l_B^2}\right)\right.\right.$$
$$\left.\left.+L_{N_c}^1\left(\frac{r^2}{2l_B^2}\right)+(N_c\rightarrow N_F)\right]\right\}^2, \quad \text{(C6)}$$

where $N\equiv 2\pi l_B^2 n(\mathbf{r})$. By using the asymptotic expression $e^{-x/2}L_{n-1}^1(x)\simeq\sqrt{n/x}J_1(2\sqrt{xn})$, where $J_1(x)$ is a Bessel function of the first kind, valid for $n\gg 1$, we obtain for N_F, $N_c\gg 1$,

$$g(r)\simeq 1-\frac{4}{N^2}[e^{-r^2/4l_B^2}+\psi(N_c,r)+\psi(N_F,r)]^2, \quad \text{(C7)}$$

where $\psi(n,r)=2nJ_1(rl_B^{-1}\sqrt{2n})/rl_B^{-1}\sqrt{n/2}$ and we have approximated $N_c-1\simeq N_c$ and $N_F-1\simeq N_F$. Using Eq. (C7) into Eq. (10), with $n(\mathbf{r})\equiv\bar{n}$ being the electron density in the isotropic case, we can obtain an expression for the exchange energy per particle in the large N_c, N_F limit with the exact solution

$$\mu^{ex}=-\frac{e^2}{\epsilon l_B}\frac{4}{3\pi}\frac{1}{N_c}\left\{4\sqrt{2}\sqrt{N_c}\left[(N_F-N_c)K\left(\frac{N_F}{N_c}\right)\right.\right.$$
$$\left.+(N_c+N_F)E\left(\frac{N_F}{N_c}\right)\right]+4\sqrt{2}(N_c^{3/2}+N_F^{3/2})$$
$$+6\pi^{3/2}e^{-N_c}N_c[I_0(N_c)+I_1(N_c)]+6\pi^{3/2}e^{-N_F}N_F[I_0(N_F)$$
$$\left.+I_1(N_F)]+\frac{3}{2\sqrt{2}}\pi^{3/2}\right\}, \quad \text{(C8)}$$

where $K(n)$ and $E(n)$ are elliptic integrals of first and second kind, respectively, and $I_n(z)$ are the modified Bessel functions of the first kind.

[1] For a recent review on graphene, see A. H. Castro Neto, F. Guinea, N. M. R. Peres, K. S. Novoselov, and A. K. Geim, Rev. Mod. Phys. **81**, 109 (2009).

[2] Z. Q. Li, E. A. Henriksen, Z. Jiang, Z. Hao, M. C. Martin, P. Kim, H. L. Stormer, and D. N. Basov, Nat. Phys. **4**, 532 (2008).

[3] J. E. Drut and T. A. Lähde, Phys. Rev. Lett. **102**, 026802 (2009).

[4] S. Sorella and E. Tosatti, Europhys. Lett. **19**, 699 (1992).

[5] I. F. Herbut, Phys. Rev. Lett. **97**, 146401 (2006).

[6] S.-S. Lee and P. A. Lee, Phys. Rev. Lett. **95**, 036403 (2005).

[7] J. González, F. Guinea, and M. A. H. Vozmediano, Nucl. Phys. B **424**, 595 (1994).

[8] Y. Barlas, T. Pereg-Barnea, M. Polini, R. Asgari, and A. H. Mac-Donald, Phys. Rev. Lett. **98**, 236601 (2007).

[9] A. Principi, M. Polini, G. Vignale, and M. I. Katsnelson, Phys. Rev. Lett. **104**, 225503 (2010).

[10] K. S. Novoselov, A. K. Geim, S. V. Morozov, D. Jiang, M. I. Katsnelson, I. V. Grigorieva, S. V. Dubonos, and A. A. Firsov, Nature (London) **438**, 197 (2005).

[11] Y. Zhang, Y.-W. Tan, H. L. Stormer, and P. Kim, Nature (London) **438**, 201 (2005).

[12] X. Du, I. Skachko, F. Duerr, A. Luican, and E. Y. Andrei, Nature (London) **462**, 192 (2009).

[13] K. I. Bolotin, F. Ghahari, M. D. Shulman, H. L. Stormer, and P. Kim, Nature (London) **462**, 196 (2009).

[14] Y. Zhang, Z. Jiang, J. P. Small, M. S. Purewal, Y.-W. Tan, M. Fazlollahi, J. D. Chudow, J. A. Jaszczak, H. L. Stormer, and P. Kim, Phys. Rev. Lett. **96**, 136806 (2006).

[15] A. J. M. Giesbers, L. A. Ponomarenko, K. S. Novoselov, A. K. Geim, M. I. Katsnelson, J. C. Maan, and U. Zeitler, Phys. Rev. B **80**, 201403 (2009).

[16] A. Iyengar, J. Wang, H. A. Fertig, and L. Brey, Phys. Rev. B **75**, 125430 (2007).

[17] Y. A. Bychkov and G. Martinez, Phys. Rev. B **77**, 125417 (2008).

[18] K. Shizuya, Phys. Rev. B **75**, 245417 (2007).

[19] M. L. Sadowski, G. Martinez, M. Potemski, C. Berger, and W. A. de Heer, Phys. Rev. Lett. **97**, 266405 (2006).

[20] Z. Jiang, E. A. Henriksen, L. C. Tung, Y.-J. Wang, M. E. Schwartz, M. Y. Han, P. Kim, and H. L. Stormer, Phys. Rev. Lett. **98**, 197403 (2007).

[21] R. S. Deacon, K.-C. Chuang, R. J. Nicholas, K. S. Novoselov, and A. K. Geim, Phys. Rev. B **76**, 081406 (2007).

[22] E. A. Henriksen, P. Cadden-Zimansky, Z. Jiang, Z. Q. Li, L.-C. Tung, M. E. Schwartz, M. Takita, Y.-J. Wang, P. Kim, and H. L. Stormer, Phys. Rev. Lett. **104**, 067404 (2010).

[23] M. Orlita and M. Potemski, Semicond. Sci. Technol. **25**, 063001 (2010).

[24] W. Kohn, Phys. Rev. **123**, 1242 (1961).

[25] C. Kallin and B. I. Halperin, Phys. Rev. B **30**, 5655 (1984).

[26] M. Dobers, K. v. Klitzing, and G. Weimann, Phys. Rev. B **38**, 5453 (1988).

[27] A. Pinczuk, B. S. Dennis, D. Heiman, C. Kallin, L. Brey, C. Tejedor, S. Schmitt-Rink, L. N. Pfeiffer, and K. W. West, Phys. Rev. Lett. **68**, 3623 (1992).

[28] L. V. Kulik, I. V. Kukushkin, V. E. Kirpichev, J. H. Smet, K. v. Klitzing, and W. Wegscheider, Phys. Rev. B **63**, 201402 (2001).

[29] A. B. Van'kov, L. V. Kulik, I. V. Kukushkin, V. E. Kirpichev, S. Dickmann, V. M. Zhilin, J. H. Smet, K. von Klitzing, and W. Wegscheider, Phys. Rev. Lett. **97**, 246801 (2006).

[30] R. Roldán, J.-N. Fuchs, and M. O. Goerbig, Phys. Rev. B **80**, 085408 (2009).

[31] R. Roldán, M. O. Goerbig, and J.-N. Fuchs, Semicond. Sci. Technol. **25**, 034005 (2010).

[32] K. Shizuya, Phys. Rev. B **81**, 075407 (2010).

[33] M. I. Katsnelson, Eur. Phys. J. B **51**, 157 (2006).

[34] T. M. Rusin and W. Zawadzki, Phys. Rev. B **78**, 125419 (2008).

[35] K. Moon, H. Mori, K. Yang, S. M. Girvin, A. H. MacDonald, L. Zheng, D. Yoshioka, and S.-C. Zhang, Phys. Rev. B **51**, 5138 (1995).

[36] B. I. Halperin and P. C. Hohenberg, Phys. Rev. **188**, 898 (1969).

[37] M. O. Goerbig, R. Moessner, and B. Douçot, Phys. Rev. B **74**, 161407(R) (2006).

[38] M. O. Goerbig, arXiv:1004.3396 (unpublished).

[39] G. F. Giuliani and G. Vignale, *Quantum Theory of the Electron Liquid* (Cambridge University Press, Cambridge, 2005).

[40] M. A. Eriksson, A. Pinczuk, B. S. Dennis, S. H. Simon, L. N. Pfeiffer, and K. W. West, Phys. Rev. Lett. **82**, 2163 (1999).

[41] N. M. R. Peres, F. Guinea, and A. H. Castro Neto, Phys. Rev. B **72**, 174406 (2005).

[42] I. L. Aleiner and L. I. Glazman, Phys. Rev. B **52**, 11296 (1995).

[43] Notice that this is also the behavior found by Aleiner and Glazman for a 2DEG at high filling factors if we replace N_c by N_F. See, e.g., Eq. (B28) of Ref. 42 where they consider a single parabolic band (no need of ultraviolet cutoff).

[44] E. H. Hwang, Ben Yu-Kuang Hu, and S. Das Sarma, Phys. Rev. Lett. **99**, 226801 (2007).

[45] J. Martin, N. Akerman, G. Ulbricht, T. Lohmann, J. H. Smet, K. V. Klitzing, and A. Yacoby, Nat. Phys. **4**, 144 (2008).

[46] J. P. Longo and C. Kallin, Phys. Rev. B **47**, 4429 (1993).